Published in final edited form as:
Brain Struct Funct. 2014 January ; 219(1): 35–47. doi:10.1007/s00429-012-0482-6.

Purkinje cell compartmentalization in the cerebellum of the spontaneous mutant mouse *dreher*

Roy V. Sillitoe[1,*], **Nicholas A. George-Jones**[1], **Kathleen J. Millen**[2], and **Richard Hawkes**[3]

[1]Department of Pathology and Immunology, Department of Neuroscience, Baylor College of Medicine, Jan and Dan Duncan Neurological Research Institute of Texas Children's Hospital, 1250 Moursund street, Suite 1325, Houston, Texas 77030, USA

[2]Seattle Children's Hospital Research Institute Center for Integrative Brain Research and The University of Washington Department of Pediatrics 1900 Ninth Avenue C9S-10 Seattle WA 98101

[3]Department of Cell Biology and Anatomy, and Hotchkiss Brain Institute, Faculty of Medicine, The University of Calgary, Calgary, Alberta T2N 4N1, Canada

Abstract

The cerebellar morphological phenotype of the spontaneous neurological mutant mouse *dreher* (*Lmx1a*$^{dr\text{-}J}$) results from cell fate changes in dorsal midline patterning involving the roof plate and rhombic lip. Positional cloning revealed that the gene *Lmx1a*, which encodes a LIM homeodomain protein, is mutated in *dreher*, and is expressed in the developing roof plate and rhombic lip. Loss of Lmx1a causes reduction of the roof plate, an important embryonic signaling center, and abnormal cell fate specification within the embryonic cerebellar rhombic lip. In adult animals, these defects result in variable, medial fusion of the cerebellar vermis and posterior cerebellar vermis hypoplasia. It is unknown whether deleting *Lmx1a* results in displacement or loss of specific lobules in the vermis. To distinguish between an ectopic and an absent vermis, the expression patterns of two Purkinje cell specific compartmentation antigens, zebrin II/aldolase C and the small heat shock protein HSP25, were analyzed in *dreher* cerebella. The data reveal that despite the reduction in volume and abnormal foliation of the cerebellum, the transverse zones and parasagittal stripe arrays characteristic of the normal vermis are present in *dreher*, but may be highly distorted. In *dreher* mutants with a severe phenotype, zebrin II stripes are fragmented and distributed non-symmetrically about the cerebellar midline. We conclude that although Purkinje cell agenesis or selective Purkinje cell death may contribute to the *dreher* phenotype, our data suggest that aberrant anlage patterning and granule cell development lead to Purkinje cell ectopia, which ultimately causes abnormal cerebellar architecture in *dreher*.

Keywords

whole mount immunohistochemistry; HSP25; zebrin II; cerebellar development; *Lmx1a*

[*]Address correspondence to Dr. R.V. Sillitoe, Department of Pathology and Immunology, Department of Neuroscience, Baylor College of Medicine, Jan and Dan Duncan Neurological Research Institute of Texas Children's Hospital, 1250 Moursund Street, Suite 1325, Houston, Texas 77030, USA, Tel: 832-824-8913, Fax: 832-825-1251, sillitoe@bcm.edu.

Introduction

The spontaneous neurological mutant *dreher* is one of many mouse models used to understand cellular behaviors during nervous system development. Positional cloning revealed that an autosomal recessive mutation in *Lmx1a*, encoding a LIM-homeodomain transcription factor, is responsible for the *dreher* phenotype (Millonig et al. 2000). The mutation results in abnormal formation of the roof plate and adjacent cerebellar rhombic lip, two structures that express *Lmx1a* during embryonic development. As a result, cerebellar development is significantly compromised (Millonig et al. 2000; Chizhikov et al. 2006; Chizhikov et al. 2010).

LIM-containing proteins play roles in tissue patterning, differentiation and morphogenetic movements (Kikuchi et al. 1997; Hobert et al. 1999; Zhao et al. 1999; Hobert and Westphal 2000; Hukriede et al. 2003; Hunter and Rhodes 2005; Matthews et al. 2008). In zebrafish, overexpression of ISLET-3 causes abnormal termination of *Wnt1*, *Engrailed2* and *Pax2* expression at the boundary between the mesencephalon and metencephalon (Kikuchi et al. 1997; Wingate and Hatten 1999). The consequent severely impaired morphogenetic movements result in the abnormal morphology of the cerebellar primordium (Kikuchi et al. 1997).

Lmx1a is expressed in the mouse embryo in roof plate progenitors and differentiating cells on the dorsal midline from E8.5 onwards (Millonig et al. 2000; Failli et al. 2002). Its expression expands into the adjacent rhombic lip by E12.5 (Chizhikov et al. 2006; Chizhikov et al. 2010). The roof plate is a transient signaling center that controls proliferation of the adjacent neuroepithelium and induces the rhombic lip. The rhombic lip gives rise to additional roof plate and granule neuron precursors, in addition to glutamatergic deep cerebellar nuclei neurons (Wang et al. 2005; Machold and Fishell 2005; Fink et al. 2006; Rose et al. 2009). Loss of *Lmx1a* in the *dreher* roof plate lineage leads to an early reduction in the size of the metencephalic roof plate, which secondarily reduces proliferation throughout the entire adjacent cerebellar zone where Purkinje cells are generated. Subsequently, by E12.5 *Lmx1a* expression expands into the rhombic lip where its expression is restricted to a population of granule cell progenitors that are fated to populate the posterior vermis. In the absence of *Lmx1a* function, these progenitors leave the rhombic lip prematurely and migrate into ectopic locations in the anterior vermis (Chizhikov et al. 2010). Cumulatively, these defects result in gross cerebellar hypoplasia and abnormalities that are concentrated medially, with the most obvious being the absence of a normal cerebellar vermis (Sekiguchi et al. 1992; Millonig et al. 2000; Chizhikov et al. 2006; Chizhikov et al. 2010).

While the effects of loss of *Lmx1a* have been described for granule cells, it remains unclear what happens to *dreher* Purkinje cells, which do not express *Lmx1a* at any stage. Here we examined the apparent absence of the vermis in *dreher*, and in particular sought to distinguish between two hypotheses – that the adult vermis is absent, or it is present but located ectopically and comprised of Purkinje cells that are patterned normally into a zonal map with distinct molecular profiles.

Materials and methods

Animals, Perfusion and Sectioning

All animal procedures conformed to institutional regulations and the *Guide to the Care and Use of Experimental Animals* from the Canadian Council for Animal Care. Breeder pairs heterozygous for the *Lmx1a* gene (B6C3Fe *a/a-Lmx1a*$^{dr\text{-}J}$) were obtained from Jackson Laboratories (Bar Harbor, Maine) and mated in our breeding colony. B6C3Fe *a/a-Lmx1a*$^{dr\text{-}J}$ contains a point mutation in the *Lmx1a* gene and is predicted to produce an altered protein that is likely to be unstable *in vivo* (Chizhikov et al. 2006). Phenotypically, homozygous mice (*Lmx1a*$^{dr\text{-}J}$*/Lmx1a*$^{dr\text{-}J}$ *= dreher*) were easily identifiable based on a white belly spot clearly evident after fur development, severe ataxia and circling behavior, and by their small size compared to littermate controls. PCR was performed according to standard protocols. Primers and conditions used in the current study are available upon request. All experiments were performed on animals that were at least 3 weeks old.

Mice were deeply anaesthetized with sodium pentobarbital (100 mg/kg, i.p.) and transcardially perfused with 0.9% NaCl in 0.1M phosphate buffer (pH 7.4) followed by 4% paraformaldehyde in 0.1M phosphate buffer (pH 7.4). The brains were then removed and post-fixed in 4% paraformaldehyde at 4°C for 48 hours. The cerebella were then cryoprotected through a series of buffered 10% (2 hrs), 20% (2 hrs), and 30% (overnight) sucrose solutions. Series of 40μm thick transverse sections were cut through the extent of the cerebellum on a cryostat and collected for free-floating immunohistochemistry.

Antibodies

Anti-zebrin II is a mouse monoclonal antibody produced by immunization with a crude cerebellar homogenate from the weakly electric fish *Apteronotus*: it was used directly from spent hybridoma culture medium at a concentration of 1:1000 (Brochu et al. 1990). On immunoblots mouse monoclonal anti-zebrin II has been shown to recognize a single polypeptide band of apparent molecular weight 36 kilodaltons (kDa) on cerebellar homogenates from all vertebrate classes studied (fish - Lannoo et al. 1991; Meek et al. 1992, birds - Pakan et al. 2007 and mammals - Sillitoe et al. 2005). As previously shown, we found that zebrin II immunoreactivity is expressed strongly in a subset of Purkinje cells (e.g. Brochu et al. 1990), and weakly in some glia (e.g., Walther et al. 1998).

Rabbit polyclonal anti-HSP25 (StressGen; Victoria, BC, Canada) was used diluted at 1:1000. On western blots of adult mouse cerebellar homogenates this rabbit polyclonal anti-HSP25 antibody recognizes a single band of approximately 25 kDa (manufacturer's data sheet and see Armstrong et al. 2000). Our studies using this antibody resulted in a tissue-staining pattern identical to that previously reported in wild type mice (Armstrong et al. 2000; Armstrong et al. 2001).

Monoclonal anti-calbindin (1:5000) is a well-established Purkinje cell specific marker and was purchased from Swant (Bellinzona, Switzerland).

Immunohistochemistry

Immunohistochemistry was carried out as described previously (Sillitoe et al. 2003). Briefly, tissue sections were washed thoroughly, blocked with 10% normal goat serum (Jackson Immunoresearch Laboratories, West Grove, PA) and then incubated in 0.1 M phosphate-buffered saline (PBS, pH 7.4, Sigma, St. Louis, MO, USA) containing 0.1% Triton-X and the primary antibody for 16-18 hours at 4°C. Secondary incubation in horseradish peroxidase-conjugated goat anti-rabbit or anti-mouse antibody (diluted 1:200 in PBS; Jackson Immunoresearch Laboratories, West Grove, PA) lasted 2 hrs at room temperature. Diaminobenzidine was used to visualize the reaction product. Sections were dehydrated through an alcohol series, cleared in xylene and cover-slipped with Entellan mounting medium (BDH Chemicals, Toronto, ON, Canada).

Photomicrographs were captured with a SPOT Cooled Color digital camera (Diagnostic Instruments Inc.) and assembled in Adobe Photoshop version 4.0. The images were cropped and corrected for brightness and contrast but not otherwise manipulated.

Whole mount immunohistochemistry

Whole mount immunostained tissue was processed according to a protocol designed to screen for patterning defects in the cerebellum of mutant mice (Sillitoe and Hawkes 2002). Briefly, cerebella were post-fixed overnight at 4°C in Dent's fixative (Dent et al. 1989). Next cerebella were incubated in Dent's bleach (Dent et al. 1989) for ∼6 hrs at room temperature, then dehydrated in 2 × 30 min each 100% methanol. The tissue was passed through 4-5 cycles of chilling to -80°C and thawing to room temperature in 100% methanol followed by overnight incubation in methanol at -80°C. Next, cerebella were rehydrated for 90 min each in 50% methanol, 15% methanol, and PBS then enzymatically digested in 10μg/ml proteinase K (>600 units/ml; Boehringer Mannheim) in PBS for 5 min at room temperature. After rinsing 3 × 30 min in PBS, the tissue was incubated in blocking buffer (Davis 1993) overnight at 4°C. The tissue was then incubated for 48-96 hrs in zebrin II antibody (1:200), rinsed 3 × 2 hrs at 4°C, and incubated for 48-72 hrs at 4°C in secondary antibody (1:200, Jackson ImmunoResearch Lab). Finally, the tissue was rinsed 4 × 3 hrs each at 4°C followed by a final overnight rinse, incubated in 0.2% bovine serum albumin, 0.1% Triton X-100 in PBS (PBT: Davis 1993) for 2 hrs at room temperature, and immunoreactivity revealed with diaminobenzidine plus 0.5 μl/ml 30% H_2O_2.

Whole mount photomicrographs were captured with a SPOT digital camera (Diagnostics Instruments, Sterling Heights, MI) mounted on a Zeiss Stemi SV6 microscope. Cerebella were photographed immersed in PBT under incident illumination. Montages were assembled in Adobe Photoshop 4.0. The images were cropped and corrected for brightness and contrast but not otherwise manipulated.

Results

Morphology of the dreher cerebellum

The cerebellum in *Lmx1a*$^{dr\text{-}J}$/*Lmx1a*$^{dr\text{-}J}$ (*dreher*) mice is markedly reduced in size (Fig. 1; Sekiguchi et al. 1992; Millonig et al. 2000). A system to grade the variable phenotype was

published by Mishima et al. (2009). We have adopted their nomenclature to characterize the *dreher* morphology in our experiments. No gross morphological abnormalities were seen in heterozygous littermates (Fig. 1B: although a heterozygous neural phenotype has been reported – Patrylo et al. 1990). The morphological abnormalities of the cerebellum in *dreher* mice range from partial fusion at the midline and mild rotation or ectopia of the vermal lobules (compare +/+ in Fig. 1A to a grade 2 *dreher* in Fig. 6; Mishima et al. 2009 and also see Fig. 9), to the complete lack of midline fusion and apparent absence of the vermis. In the more severe cases, only a few lobules are present, located laterally, and the failure of midline fusion creates an acortical crevice that exposes the fourth ventricle (grade 4 *dreher* in Fig. 1C). The variability within the *dreher* phenotype may be due to differential modifier gene effects on mixed genetic backgrounds (Murcia et al. 2007; Mishima et al. 2009).

Histology of the dreher cerebellum

Despite the severe defects in lobulation and the dramatic reduction in the size of individual lobules, cerebellar lamination appears normal in *dreher* (Fig. 2; Sekiguchi et al. 1992; Chizhikov et al. 2010 and unpublished data). However, the granular layer has an irregular thickness with the thinnest regions observed in the vermis (arrowheads in Fig. 3C and Fig. 6D). Most Purkinje cells in the adult *dreher* cerebellum are organized into a normal monolayer as seen by the expression of calbindin, zebrin II and HSP25 (see Fig. 3 and Fig. 7), but in amongst the cerebellar nuclei (CN) clusters of ectopic zebrin II-immunoreactive Purkinje cells are common (compare lateral nuclei in Fig. 2A with 2B; see also Fig 2C). In addition, ectopic HSP25-immunoreactive Purkinje cells were found within the white matter (arrow Fig. 2D). Furthermore, calbindin immunoreactivity also revealed ectopic Purkinje cells within the white matter and CN (compare Fig 2E with 2F). Interestingly, mild lamination defects have also been observed in the *dreher* cerebral cortex (Costa et al. 2001) and hippocampus (Sekiguchi et al. 1992).

Organization of the vermis

The fundamental parcellation of the mammalian cerebellar vermis appears to be into four transverse zones - the anterior zone (AZ: ∼ lobules I-V), the central zone (CZ: ∼lobules VI, VII), the posterior zone (PZ: ∼lobules VIII) and the nodular zone (NZ: ∼lobule IX, X) (Ozol et al. 1999; Apps and Hawkes 2009). The zebrin II/aldolase C expression pattern in Purkinje cells reveals that the AZ and PZ are further subdivided, from medial to lateral, into an array of at least seven parasagittal stripes designated P1+ - P7+ (for zebrin II-immunopositive) and P1- to P7- (for zebrin II-immunonegative). While all Purkinje cells in the rodent CZ and the NZ express zebrin II, the small heat shock protein HSP25 reveals a pattern of Purkinje cell stripes that respect the anterior-posterior limits delineated by the transverse zones (Armstrong et al. 2000; Armstrong and Hawkes 2002). The expression of HSP25 reveals at least five immunoreactive stripes in the CZ and at least three thick immunoreactive stripes in the NZ (Armstrong et al. 2000). Using these markers of Purkinje cell patterning we conclude that the four transverse zones of the adult vermis are present in *dreher*, but are ectopically located laterally. Because the expression of these markers is refractory to Purkinje cell ectopia and experimental manipulations, they can be used to identify the cerebellar vermis in ectopic locations (reviewed in Armstrong and Hawkes 2000; Sillitoe and Hawkes 2002).

Anterior zone—In the AZ of control mice, a highly reproducible array of zebrin II immunoreactive stripes is present (Ozol et al. 1999; Sillitoe and Hawkes 2002; Fig. 3). At the midline, P1+ is thin and distinct in all five lobules of the AZ. Laterally on either side of the midline, P2+ to P4+ are arranged symmetrically. The P2+ stripe does not extend caudally far beyond the primary fissure and is restricted to lobules IV and V (see also rabbit - Sanchez et al. 2002; guinea pig - Larouche et al. 2003). The P3+ stripe is distinct in all five lobules and is situated approximately 500μm lateral to P1+ in lobules I-III (Fig. 3A; Sillitoe and Hawkes 2002). The most lateral stripe, P4+, is visible in all lobules of the AZ and is most clearly seen on wholemount immunoperoxidase-stained cerebella (e.g., Sillitoe and Hawkes 2002).

The lobules of the AZ in *dreher* are often rotated with respect to the posterior lobules and ectopic with respect to the midline (e.g., arrow - Fig. 3B showing a grade 3 *dreher* cerebellum). Although deflected, P1+ to P3+ can be confidently identified in the *dreher* AZ (Figs. 3C, D: the +/+ midline P1+ stripe is derived from the fusion of the stripes from each hemicerebellum and hence is represented separately in the two ectopic halves). The abnormalities in Purkinje cell patterning appear to be consistent with the rotated morphology of the lobules. Stripes in the AZ are often positioned such that they are rotated in the same direction as the lobules they traverse (Fig. 3C and D). Thus, despite the severely convoluted morphology of the AZ, the underlying pattern of zebrin II is relatively normal in *dreher*. However, the distance between P1+ and P3+ is approximately half the distance than it is in +/+ littermates (∼250 μm in a grade 3 *dreher* compared to ∼500 μm in +/+ for lobule IV). Moreover, in *dreher* the distance between P1+ and P3+ is highly variable between the ventral (lobules I-III) and dorsal (lobules IV and V) sub-divisions of the AZ (Fig. 3).

Central zone—The alternating zebrin II+/- stripes seen in the +/+ AZ disappear in the CZ, which begins caudal to the primary fissure (Ozol et al. 1999). All Purkinje cells in the vermis of wild type mice CZ express zebrin II (Fig. 4A; Ozol et al. 1999). As was the case for the AZ, the *dreher* CZ is in an ectopic location lateral to the cerebellar midline. In *dreher* mutants with milder phenotypes, lobules VI-VII are rotated in the horizontal plane such that they are only partially located at the midline (grade 2 *dreher* cerebellum in Fig 4D). In the more severe cases, lobules VI-VII are no longer visible at the midline and a large gap separates the two sides of the cerebellum (e.g., grade 4 *dreher* in Fig. 1C). Adjacent to the midline gap, a region that expresses zebrin II uniformly can reliably be identified (Figs. 4B and C). This is consistent with the presence of an ectopic CZ domain, but cannot be distinguished by zebrin II expression from the uniformly zebrin II+ crus I lobule of the hemispheres (especially as hemispheric lobulation is also abnormal).

The CZ of the +/+ vermis contains five parasagittal stripes of Purkinje cells that express HSP25 – one astride the midline and two laterally on either side (Fig. 5A: Armstrong et al. 2000). No HSP25-immunoreactive Purkinje cells are present in the hemispheres. (Ectopic HSP25-expression in Purkinje cells is occasionally seen in mutant mice, for example in an NPC1 mouse model of Niemann-Pick type C disease - Sarna et al. 2003 - but these are infrequent and not organized in stripes). HSP25 immunoreactivity was therefore used to determine whether the CZ vermis in *dreher* is genetically ablated or located ectopically. Immunohistochemical analysis reveals that a variable, fragmented pattern of HSP25 is

present in the *dreher* CZ (compare near adjacent tissue sections in a grade 4 mutant in Figs. 5B and C). On each tissue section individual stripes of HSP25-immunoreactive Purkinje cells (Fig. 5D) were often observed in isolation, with few or no adjacent stripes (Fig. 5B and C). Thus, the unambiguous identification of all five HSP25 immunoreactive stripes is difficult in the *dreher* CZ. This is likely due in part to the ectopia of HSP25+ Purkinje cells (Fig. 2C). In addition however, the deflection of each side of the unpaired vermis appears to cause an anterior-posterior staggering of Purkinje cell stripes on one side of the vermis relative to the other.

Posterior zone—In wild type cerebella (Figs. 6A and C), a pattern of alternating zebrin II +/- stripes is seen in the PZ (e.g., lobule VIIII; rat - Hawkes and Leclerc 1987; mouse - Eisenman and Hawkes 1993; Ozol et al. 1999; Sillitoe and Hawkes 2002: reviewed in Marzban and Hawkes 2010). The characteristic saddle shape of lobule VIII in the +/+ cerebellum (Figs. 1A, 6C) is often difficult to identify in *dreher* and, as is the case for the anterior lobules, the PZ is skewed laterally (grade 2 *dreher* cerebellum in Fig. 6B) and partially concealed by the hemispheric lobules (Fig. 6D). Nevertheless, the P1+ to P4+ stripes of the PZ vermis can each be identified in *dreher* (Fig 6B and Fig. 6E), although often with poor symmetry between the two sides of the cerebellum (e.g. zebrin II-immunoreactive stripes are obvious on the right side of the cerebellum in Fig. 6B but poorly resolved on the left side). One feature we observed in some mutants was the lack of tissue continuity at the apex of lobule IX (black asterisk in a grade 3 mutant shown in Fig. 6E). This conspicuous gap in the tissue was consistent with a morphological defect at the midline. In such mutants we used this location as a landmark to locate the midline zebrin II stripe and accordingly, the adjacent non-symmetrical stripes (Fig. 6E).

Nodular Zone—In the most posterior lobules of the +/+ vermis, the zebrin II-immunonegative stripes disappear as the PZ gives way to the NZ (~ lobules IX and X; Ozol et al. 1999), and almost all Purkinje cells express zebrin II (see Fig. 6A). Whole mount and serial section analyses of *dreher* cerebella confirmed the presence of the NZ as defined by the uniform expression of zebrin II (see Figs. 6B and D). The distribution of NZ Purkinje cells that express HSP25 in *dreher* revealed an array of stripes characteristic of lobules IX and X (Fig. 7). For example, in lobule IX at least five obvious stripes are revealed in wild type and *dreher* mutants (arrows Fig. 7A, B). However, in *dreher* the abnormal foliation causes the regular array of stripes to be deflected laterally, which ultimately results in a mis-alignment of stripes between the rostral and caudal faces of the lobule (asterisk in Fig. 7B).

Organization of the hemispheres

Zebrin II expression in the hemispheres revealed alternating stripes in all specimens despite the severe lobulation abnormalities. In +/+ cerebella, at least four prominent zebrin II+ stripes occupy the hemispheres (P4a+, P5b+, P6+ and P7+: Fig. 8A). Strikingly, in *dreher* the pattern of zebrin II expression in the hemispheres is more or less normal in both the anterior and the posterior hemispheres. The parasagittal pattern in (presumptive) HVI gives way to the uniform zebrin II expression in crus I (Fig. 8B). In crus II and the paramedian lobule (Fig. 8B) all four zebrin II immunoreactive stripes were observed and easily traced over the cerebellar surface.

In wild type mice all Purkinje cells are zebrin II immunoreactive in the flocculus and the paraflocculus (Fig. 8C), but HSP25 reveals a heterogeneous pattern in the paraflocculus (Fig. 8E; Armstrong et al. 2000). Similarly, in *dreher* the expression of zebrin II is uniform in the flocculus (Fig. 8D) while HSP25 is striped in the paraflocculus (Fig. 8F).

Discussion

Several developmental defects could account for the cerebellar abnormalities in *dreher*. These include agenesis of the vermis, formation of the vermis followed by cell death and ectopia of the vermis due to abnormal Purkinje cell migration and/or failure of midline fusion. Our data are consistent with the hypothesis that Purkinje cells from all four zones of the vermis are present in *dreher* but are displaced laterally to ectopic locations due to a failure of midline fusion (Fig. 9). The presumptive ectopic vermis is reliably distinguished from the hemispheres on several grounds: as in wild type mice, the zebrin II and HSP25 expression patterns in *dreher* define distinct subsets of Purkinje cells; the individual hemispheric zebrin II Purkinje cell stripes can be identified; and there are no HSP25+ stripes in the hemispheres of adult wild type mice. Furthermore, based on Purkinje cell phenotypes, our data also suggest that some Purkinje cell ectopia in *dreher* is due to the failure of embryonic Purkinje cell clusters to disperse properly.

Several previous investigations have provided evidence that Purkinje cell stripe markers are expressed with fidelity despite Purkinje cell ectopia and in the presence of abnormal connectivity. For zebrin II these include studies of mutant mice with cerebellar developmental abnormalities (e.g., *reeler* – Edwards et al. 1994; *disabled* – Gallagher et al. 1998), studies of afferent lesions (e.g., Leclerc et al. 1988; Ji and Hawkes 1995; Zagrebelsky et al. 1996; Armstrong et al. 2000), and studies in which the cerebellum is grown in slice cultures (Seil et al. 1995) or as intracortical or intraocular grafts (Wassef et al. 1990). For constitutive HSP25 expression, they include various lesion paradigms (afferent ablations, eye sutures etc.: Armstrong et al. 2000, Armstrong et al. 2001) and studies of mouse cerebellar mutants (*weaver* – Armstrong and Hawkes 2001; *disabled* – Armstrong et al. 2009). Thus, we conclude that examination of Purkinje cell expression patterns is a valid approach to examine cerebellar patterning in *dreher* mice.

Zebrin II expression revealed that in *dreher* mice Purkinje cell stripes are either altered in width or the spacing between stripes is severely reduced (see Fig. 2 and Fig. 3). The reduction in the number of zebrin II+ cells per stripe could be due to the failure of specific embryonic Purkinje cell clusters to disperse into stripes (Fig. 2). Similarly, the reduced spacing between zebrin II+ stripes could reflect a failure of Purkinje cell subsets to properly incorporate into the Purkinje cell layer (Fig. 3). Indeed, previous work has shown that *cerebellar deficient folia* (*cdf*) mutants have a selective failure of a zebrin II- Purkinje cell subset to disperse, which ultimately results in stripe width abnormalities (Beierbach et al. 2001). However, in contrast to *cdf*, Purkinje cell ectopia in *dreher* mice likely involves multiple subsets (Fig. 2). Purkinje cell clusters are known to disperse under the control of the reelin-disabled signaling pathway (E18-P3: reviewed in Howell et al. 1997; Larouche and Hawkes 2006; Larouche et al. 2008; Miyata et al. 2010). We propose that in *dreher*, the lack of reelin signaling medially could in theory result in a failure of vermis Purkinje cells to

disperse properly. The absence of this key cell migration signal might explain why some Purkinje cells are ectopic and trapped among the cerebellar nuclei, a potent source of reelin in the developing cerebellum (Jensen et al. 2002).

It is also likely that fewer Purkinje cells are generated in *dreher* mice due to reduced mitogenic signaling from a reduced roof plate (Chizhikov et al. 2006; Chizhikov et al. 2010). Moreover, loss of *Lmx1a* may affect specific subsets of Purkinje cells more than others. For example, removal of *Engrailed1* causes severe defects in the patterning of zebrin II stripes, whereas loss of *Engrailed2* function causes major alterations in HSP25 stripe patterning (Sillitoe et al. 2008). In addition, several spontaneous and engineered mutations that affect cerebellar development induce selective Purkinje cell ectopia (Armstrong and Hawkes 2001; Beierbach et al. 2001; Larouche et al. 2008). Moreover, genetic and physical insults to the developing cerebellum cause patterned Purkinje cell death (Sarna and Hawkes 2003). Similar differential alterations in the pattern of specific Purkinje cell stripes or subsets may also be true in *dreher*.

Since *Lmx1a* is not expressed in Purkinje cells at any stage of their development, all vermis defects must be secondary to roof plate and rhombic lip abnormalities in *dreher* mice. The complexity of the *dreher* phenotype may be best understood from the perspective of the normal developmental dynamics of the developing cerebellum. First, in contrast to the theory of fusion of the hemi-cerebella to form the whole structure (Louvi et al. 2003), recent genetic fate mapping data supports a model where initially only the anterior vermis is fused and cell proliferation allows for expansion and development of more posterior vermis (Sgaier et al. 2005; Sillitoe and Joyner 2007). Second, during vermis expansion the initially wing-like cerebellum rotates ∼90 degrees and transforms the anterior-posterior axis into the medial-lateral axis of the cerebellum (Fig. 9; Sgaier et al. 2005; Sillitoe and Joyner 2007). Since the anterior vermis is initially unaffected by the *dreher* mutation (Chizhikov et al. 2010), cell proliferation and tissue expansion appear to be spared in the anterior cerebellum of *dreher* and therefore patterning of Purkinje cell stripes proceeds normally in this domain (Fig. 9). Further, we conclude that anterior midline fusion is also less dependent on *Lmx1a* function in this domain. Posterior predominant vermis hypoplasia is at least partially explained by a switch in the fate of posterior granule cells to anterior domains (Chizhikov et al. 2010). However, since the roof plate provides mitogenic signals that affect Purkinje cell neurogenesis, posterior vermis proliferation is likely compromised. In severe cases of *dreher* (grades 3-5) the two halves of the vermis are often deflected from the midline by ∼45 degrees (e.g. lobule HVI in Fig. 1B). We speculate that in addition to vermis expansion, *Lmx1a* is required for rotation of the hemi-cerebella and formation of the mature medial-lateral axis. It is intriguing that expansion and rotation of the vermis might be tightly coupled (and linked by *Lmx1a* function) but independent of Purkinje cell stripe patterning.

Cerebellar abnormalities predominant in the vermis are seen in several rodent models. The best-known mouse example is the *weaver* (*wv*/+) mouse, in which neuronal migration defects – directly affecting both granule cells (Hatten et al. 1986; Goldowitz 1989) and Purkinje cells (Smeyne and Goldowitz 1990) – lead to lobule malformations that are both regionalized (e.g., specific abnormalities in the CZ: Armstrong and Hawkes 2001) and most severe in the vermis (e.g. Rezai and Yoon 1972; Blatt and Eisenman 1985; Herrup and

Trenkner 1987). Similarly, the hereditary cerebellar vermis defect rat (cvd), which lacks the Netrin-1 receptor Unc5h3, is characterized by defects in the cerebellar vermis and a dysplastic cerebellum (Kuwamura et al. 1997; Kuramoto et al. 2004). At around E19, cvd rats lack normal vermis development and subsequently the cerebellar hemispheres appear fused. Lamination is abnormal and the Bergmann glia and Purkinje cells are abnormally oriented (Kuwamura et al. 1997). It is interesting to speculate that an important cause of abnormal cerebellar morphology in all three mutations may be a direct consequence of compromised granule cell development leading to abnormal midline fusion. Because the expression of compartmentation antigens has not been analyzed in cvd rats, it remains a possibility that their vermis is also positioned ectopically within the hemispheres.

Several congenital malformations in humans also affect the genesis of the cerebellar vermis. For example, heterozygous mutations in *ZIC1* and *ZIC4* and heterozygous mutations of *FOXC1* are associated with Dandy-Walker malformation (Grinberg et al. 2004; Aldinger et al. 2009). Dandy-Walker malformation consists of either partial or complete agenesis of the vermis, in which the posterior lobules appear to be disproportionately targeted (Patel and Barkovich 2002; Barkovich et al. 2009). In addition, mutations in several cilia and basal body protein encoding genes have all recently linked to Joubert syndrome (Doherty 2009; Lee and Gleeson 2010). Joubert syndrome is associated with posterior fossa abnormalities and consists of posterior predominant vermian hypoplasia (Maria et al. 1997). Although the specific genes that are mutated in each disease are different, common underlying cellular defects may link the different conditions. Interestingly, the developmental pathogenesis of Dandy Walker malformation has been associated with abnormal rhombic lip and EGL formation (Aldinger et al. 2009; Blank et al. 2011) and EGL proliferative defects have also been hypothesized to underlie the Joubert Syndrome phenotype (Chizhikov et al. 2007; Spassky et al. 2008). Based upon the morphological abnormalities of the cerebellum, we propose that the *Lmx1a* mutation in *dreher* is a valuable animal model for understanding the developmental origins of diseases that affect the cerebellar vermis.

Acknowledgments

These studies were supported by grants from the Canadian Institutes of Health Research (RH), the CIHR Training Program in Genetics, Child Development and Health (RVS), and NIH R01 NS050386 (KJM). RVS is currently supported by new investigator start-up funds from Baylor College of Medicine and Texas Children's Hospital, by the Caroline Wiess Law Fund for Research in Molecular Medicine, a BCM IDDRC Project Development Award, and by a BCM IDDRC Grant (Number 5P30HD024064) from the Eunice Kennedy Shriver National Institute Of Child Health & Human Development.

Literature cited

Ahn AH, Dziennis S, Hawkes R, Herrup K. The cloning of zebrin II reveals its identity with aldolase C. Development. 1994; 120(8):2081–2090. [PubMed: 7925012]

Aldinger KA, Lehmann OJ, Hudgins L, Chizhikov VV, Bassuk AG, Ades LC, Krantz ID, Dobyns WB, Millen KJ. FOXC1 is required for normal cerebellar development and is a major contributor to chromosome 6p25.3 Dandy-Walker malformation. Nat Genet. 2009; 41(9):1037–1042. [PubMed: 19668217]

Apps R, Hawkes R. Cerebellar cortical organization: a one-map hypothesis. Nature Rev Neurosci. 2009; 10(9):670–681. [PubMed: 19693030]

Armstrong CL, Chung SH, Armstrong JN, Hochgeschwender U, Jeong YG, Hawkes R. A novel somatostatin-immunoreactive mossy fiber pathway associated with HSP25-immunoreactive

purkinje cell stripes in the mouse cerebellum. J Comp Neurol. 2009; 517(4):524–538. [PubMed: 19795496]

Armstrong CL, Hawkes R. Pattern formation in the cerebellar cortex. Biochem Cell Biol. 2000; 78(5): 551–562. [PubMed: 11103945]

Armstrong CL, Hawkes R. Selective Purkinje cell ectopia in the cerebellum of the *weaver* mouse. J Comp Neurol. 2001; 439(2):151–161. [PubMed: 11596045]

Armstrong CL, Krueger-Naug AM, Currie RW, Hawkes R. Constitutive expression of the 25 kDa heat shock protein Hsp25 reveals novel parasagittal bands of Purkinje cells in the adult mouse cerebellar cortex. J Comp Neurol. 2000; 416(3):383–397. [PubMed: 10602096]

Barkovich AJ, Millen KJ, Dobyns WB. A developmental and genetic classification for midbrain-hindbrain malformations. Brain. 2009; 132(Pt 12):3199–3230. [PubMed: 19933510]

Beierbach E, Park C, Ackerman SL, Goldowitz D, Hawkes R. Abnormal dispersion of a Purkinje cell subset in the mouse mutant cerebellar deficient folia (cdf). J Comp Neurol. 2001; 436(1):42–51. [PubMed: 11413545]

Bergstrom DE, Gagnon LH, Eicher EM. Genetic and physical mapping of the *dreher* locus on mouse chromosome 1. Genomics. 1999; 59(3):291–299. [PubMed: 10444330]

Blatt GJ, Eisenman LM. A qualitative and quantitative light microscopic study of the inferior olivary complex of normal, *reeler*, and *weaver* mutant mice. J Comp Neurol. 1985; 232(1):117–128. [PubMed: 3973080]

Blank MC, Grinberg I, Aryee E, Laliberte C, Chizhikov VV, Henkelman RM, Millen KJ. Multiple cerebellar developmental programs are altered by loss of Zic1 and Zic4 to cause Dandy-Walker malformation cerebellar pathogenesis. Development. 2011; 138(6):1207–1216. [PubMed: 21307096]

Brochu G, Maler L, Hawkes R. Zebrin II: A polypeptide antigen expressed selectively by Purkinje cells reveals compartments in rat and fish cerebellum. J Comp Neurol. 1990; 291(4):538–552. [PubMed: 2329190]

Chen S, Hillman DE. Developmental factors related to abnormal cerebellar foliation induced by methylazoxymethanol acetate (MAM). Brain Res. 1988; 468(2):201–212. [PubMed: 3382957]

Chizhikov V, Steshina E, Roberts R, Ilkin Y, Washburn L, Millen KJ. Molecular definition of an allelic series of mutations disrupting the mouse Lmx1a (dreher) gene. Mamm Genome. 2006; 17(10):1025–1032. [PubMed: 17019651]

Chizhikov VV, Lindgren AG, Mishima Y, Roberts RW, Aldinger KA, Miesegaes GR, Currle DS, Monuki ES, Millen KJ. Lmx1a regulates fates and location of cells originating from the cerebellar rhombic lip and telencephalic cortical hem. Proc Natl Acad Sci U S A. 2010; 107(23):10725–10730. [PubMed: 20498066]

Costa C, Harding B, Copp AJ. Neuronal migration defects in the Dreher (Lmx1a) mutant mouse: role of disorders of the glial limiting membrane. Cereb Cortex. 2001; 11(6):498–505. [PubMed: 11375911]

Davis CA. Whole-mount immunohistochemistry. Methods Enzymol. 1993; 225:502–516. [PubMed: 8231871]

Dent JA, Paulson AG, Klymkowsky MW. Whole-mount immunocytochemical analysis of the expression of the intermediate filament protein vimentin in Xenopus. Development. 1989; 105(1): 61–74. [PubMed: 2806118]

Doherty D. Joubert syndrome: insights into brain development, cilium biology, and complex disease. Semin Pediatr Neurol. 2009; 16(3):143–154. [PubMed: 19778711]

Edwards MA, Leclerc N, Crandall JE, Yamamoto M. Purkinje cell compartments in the *reeler* mutant mouse as revealed by zebrin II and 90-acetylated glycolipid antigen expression. Anat Embryol (Berlin). 1994; 190(5):417–428. [PubMed: 7887492]

Eisenman LM, Hawkes R. Antigenic compartmentation in the mouse cerebellar cortex: zebrin and HNK-1 reveal a complex, overlapping molecular topography. J Comp Neurol. 1993; 335(4):586–605. [PubMed: 7693775]

Failli V, Bachy I, Retaux S. Expression of the LIM-homeodomain gene Lmx1a (dreher) during development of the mouse nervous system. Mech Dev. 2002; 118(1-2):225–228. [PubMed: 12351192]

Failli V, Rogard M, Mattei MG, Vernier P, Retaux S. Lhx9 and Lhx9alpha LIM-homeodomain factors: genomic structure, expression patterns, chromosomal localization, and phylogenetic analysis. Genomics. 2000; 64(3):307–317. [PubMed: 10756098]

Fink AJ, Englund C, Daza RA, Pham D, Lau C, Nivison M, Kowalczyk T, Hevner RF. Development of the deep cerebellar nuclei: transcription factors and cell migration from the rhombic lip. J Neurosci. 2006; 26(11):3066–3076. [PubMed: 16540585]

Gallagher E, Howell BW, Soriano P, Cooper JA, Hawkes R. Cerebellar abnormalities in the *disabled* (mdab1-1) mouse. J Comp Neurol. 1998; 402(2):238–251. [PubMed: 9845246]

Grinberg I, Northrup H, Ardinger H, Prasad C, Dobyns WB, Millen KJ. Heterozygous deletion of the linked genes ZIC1 and ZIC4 is involved in Dandy-Walker malformation. Nat Genet. 2004; 36(10): 1053–1055. [PubMed: 15338008]

Goldowitz D. The *weaver* granuloprival phenotype is due to intrinsic action of the mutant locus in the granule cell: evidence from homozygous *weaver* chimeras. Neuron. 1989; 2(6):1565–1575. [PubMed: 2627379]

Goldowitz D, Hamre K. The cells and molecules that make a cerebellum. Trends Neurosci. 1998; 21(9):375–382. [PubMed: 9735945]

Harris MJ, Juriloff DM, Gunn TM, Miller JE. Development of the cerebellar defect in ataxic SELH/Bc mice. Teratology. 1994; 50(1):63–73. [PubMed: 7974256]

Hatten ME. Central nervous system neuronal migration. Ann Rev Neurosci. 1999; 22:511–539. [PubMed: 10202547]

Hatten ME, Liem RKH, Mason CA. *Weaver* mouse cerebellar granule neurons fail to migrate on wild type astroglial processes *in vitro*. J Neurosci. 1986; 6(9):2676–2683. [PubMed: 3528411]

Hawkes R. An anatomical model of cerebellar modules. Prog Brain Res. 1997; 114:39–52. [PubMed: 9193137]

Hawkes R, Eisenman LM. Stripes and zones: the origins of regionalization of the adult cerebellum. Perspect Dev Neurobiol. 1997; 5(1):95–105. [PubMed: 9509521]

Hawkes R, Gravel C. The modular cerebellum. Prog Neurobiol. 1991; 36(4):309–327. [PubMed: 1871318]

Hawkes R, Leclerc N. Antigenic map of the rat cerebellar cortex: the distribution of parasagittal bands as revealed by monoclonal anti-Purkinje cell antibody mabQ113. J Comp Neurol. 1987; 256(1): 29–41. [PubMed: 3546410]

Herrup K, Trenkner E. Regional differences in cytoarchitecture of the *weaver* cerebellum suggest a new model for *weaver* gene action. Neuroscience. 1987; 23(3):871–885. [PubMed: 3437994]

Hobert O, Tessmar K, Ruvkun G. The *Caenorhabditis elegans* lim-6 LIM homeobox gene regulates neurite outgrowth and function of particular GABAergic neurons. Development. 1999; 126(7): 1547–1562. [PubMed: 10068647]

Hobert O, Westphal H. Functions of LIM-homeobox genes. Trends Genet. 2000; 16(2):75–83. [PubMed: 10652534]

Howell BW, Hawkes R, Soriano P, Cooper JA. Neuronal position in the developing brain is regulated by mouse disabled-1. Nature. 1997; 389(6652):733–777. [PubMed: 9338785]

Hukriede NA, Tsang TE, Habas R, Khoo PL, Steiner K, Weeks DL, Tam PP, Dawid IB. Conserved requirement of Lim1 function for cell movements during gastrulation. Dev Cell. 2003; 4(1):83–94. [PubMed: 12530965]

Hunter CS, Rhodes SJ. LIM-homeodomain genes in mammalian development and human disease. Mol Biol Rep. 2005; 32(2):67–77. [PubMed: 16022279]

Jensen P, Zoghbi HY, Goldowitz D. Dissection of the cellular and molecular events that position cerebellar Purkinje cells: a study of the math1 null-mutant mouse. J Neurosci. 2002; 22(18):8110–8116. [PubMed: 12223565]

Ji Z, Hawkes R. Developing mossy fiber terminal fields in the rat cerebellar cortex may segregate because of Purkinje cell compartmentation and not competition. J Comp Neurol. 1995; 359(2): 197–212. [PubMed: 7499524]

Jones M, Yang M, Mickelsen O. Effects of methylazoxymethanol glucoside and methylazoxymethanol acetate on the cerebellum of the postnatal Swiss albino mouse. Fed Proc. 1972; 31(5):1508–1511. [PubMed: 5056175]

Kikuchi Y, Segawa H, Tokumoto M, Tsubokawa T, Hotta Y, Uyemura K, Okamoto H. Ocular and cerebellar defects in zebrafish induced by overexpression of the LIM domains of the islet-3 LIM/homeodomain protein. Neuron. 1997; 18(3):369–382. [PubMed: 9115732]

Kuramoto T, Kuwamura M, Serikawa T. Rat neurological mutations cerebellar vermis defect and hobble are caused by mutations in the netrin-1 receptor gene Unc5h3. Brain Res Mol Brain Res. 2004; 122(2):103–108. [PubMed: 15010202]

Kuwamura M, Ishida A, Yamate J, Kato K, Kotani T, Sakuma S. Chronological and immunohistochemical observations of cerebellar dysplasia and vermis defect in the hereditary cerebellar vermis defect (CVD) rat. Acta Neuropathol. 1997; 94(6):549–556. [PubMed: 9444356]

Lannoo MJ, Brochu G, Maler L, Hawkes R. Zebrin II immunoreactivity in the rat and in the weakly electric teleost *Eigenmannia* (Gymnotiformes) reveals three modes of Purkinje cell development. J Comp Neurol. 1991; 310(2):215–233. [PubMed: 1955583]

Larouche M, Beffert U, Herz J, Hawkes R. The Reelin receptors Apoer2 and Vldlr coordinate the patterning of Purkinje cell topography in the developing mouse cerebellum. PLoS ONE. 2008; 3(2):e1653. [PubMed: 18301736]

Larouche M, Diep C, Sillitoe RV, Hawkes R. The topographical anatomy of the cerebellum in the guinea pig, *Cavia porcellus*. Brain Res. 2003; 965(1-2):159–169. [PubMed: 12591133]

Larouche M, Hawkes R. From clusters to stripes: the developmental origins of adult cerebellar compartmentation. Cerebellum. 2006; 5(2):77–88. [PubMed: 16818382]

Leclerc N, Gravel C, Hawkes R. Development of parasagittal zonation in the rat cerebellar cortex: mabQ113 antigenic bands are created postnatally by the suppression of antigen expression in a subset of Purkinje cells. J Comp Neurol. 1988; 273(3):399–420. [PubMed: 2463281]

Lee JH, Gleeson JG. The role of primary cilia in neuronal function. Neurobiol Dis. 2010; 38(2):167–172. [PubMed: 20097287]

Louvi A, Alexandre P, Métin C, Wurst W, Wassef M. The isthmic neuroepithelium is essential for cerebellar midline fusion. Development. 2003; 130(22):5319–5330. [PubMed: 14507778]

Machold R, Fishell G. Math1 is expressed in temporally discrete pools of cerebellar rhombic-lip neural progenitors. Neuron. 2005; 48(1):17–24. [PubMed: 16202705]

Manzanares M, Trainor PA, Ariza-McNaughton L, Nonchev S, Krumlauf R. Dorsal patterning defects in the hindbrain, roof plate and skeleton in the *dreher* (dr(J)) mouse mutant. Mech Dev. 2000; 94(1-2):147–156. [PubMed: 10842066]

Maria BL, Hoang KB, Tusa RJ, Mancuso AA, Hamed LM, Quisling RG, Hove MT, Fennell EB, Booth-Jones M, Ringdahl DM, Yachnis AT, Creel G, Frerking B. “Joubert syndrome” revisited: key ocular motor signs with magnetic resonance imaging correlation. J Child Neurol. 1997; 12(7):423–430. [PubMed: 9373798]

Marzban H, Hawkes R. On the architecture of the posterior zone of the cerebellum. Cerebellum. 2011; 10(3):422–434. [PubMed: 20838950]

Matthews JM, Bhati M, Craig VJ, Deane JE, Jeffries C, Lee C, Nancarrow AL, Ryan DP, Sunde M. Competition between LIM-binding domains. Biochem Soc Trans. 2008; 36(Pt 6):1393–1397. [PubMed: 19021562]

Meek J, Hafmans TG, Maler L, Hawkes R. Distribution of zebrin II in the gigantocerebellum of the mormyrid fish *Gnathonemus petersii* compared with other teleosts. J Comp Neurol. 1992; 316(1):17–31. [PubMed: 1573049]

Miale I, Sidman RL. An autoradiographic analysis of histogenesis in the mouse cerebellum. Exp Neurol. 1961; 4:277–296. [PubMed: 14473282]

Millonig JH, Millen KJ, Hatten ME. The mouse *Dreher* gene *Lmx1a* controls formation of the roof plate in the vertebrate CNS. Nature. 2000; 403(6771):764–769. [PubMed: 10693804]

Mishima Y, Lindgren AG, Chizhikov VV, Johnson RL, Millen KJ. Overlapping function of Lmx1a and Lmx1b in anterior hindbrain roof plate formation and cerebellar growth. J Neurosci. 2009; 29(36):11377–11384. [PubMed: 19741143]

Miyata T, Ono Y, Okamoto M, Masaoka M, Sakakibara A, Kawaguchi A, Mitsuhiro M, Ogawa M. Migration, early axonogenesis, and Reelin-dependent layer-forming behavior of early/posterior-born Purkinje cells in the developing mouse lateral cerebellum. Neural Dev. 2010; 5:23. [PubMed: 20809939]

Murcia CL, Gulden FO, Cherosky NA, Herrup K. A genetic study of the suppressors of the Engrailed-1 cerebellar phenotype. Brain Res. 2007; 1140:170–178. [PubMed: 16884697]

Ozol K, Hayden JM, Oberdick J, Hawkes R. Transverse zones in the vermis of the mouse cerebellum. J Comp Neurol. 1999; 412(1):95–111. [PubMed: 10440712]

Pakan JM, Iwaniuk AN, Wylie DR, Hawkes R, Marzban H. Purkinje cell compartmentation as revealed by zebrin II expression in the cerebellar cortex of pigeons (*Columba livia*). J Comp Neurol. 2007; 501(4):619–630. [PubMed: 17278140]

Patel S, Barkovich AJ. Analysis and classification of cerebellar malformations. Am J Neuroradiol. 2002; 23(7):1074–1087. [PubMed: 12169461]

Patrylo PR, Sekiguchi M, Nowakowski RS. Heterozygote effects in dreher mice. J Neurogenet. 1990; 6(3):173–181. [PubMed: 2358966]

Rezai Z, Yoon CH. Abnormal rate of granule cell migration in the cerebellum of “weaver” mutant mice. Dev Biol. 1972; 29(1):17–26. [PubMed: 4561458]

Rose MF, Ahmad KA, Thaller C, Zoghbi HY. Excitatory neurons of the proprioceptive, interoceptive, and arousal hindbrain networks share a developmental requirement for Math1. Proc Natl Acad Sci U S A. 2009; 106(52):22462–22467. [PubMed: 20080794]

Sarna JR, Hawkes R. Patterned Purkinje cell death in the cerebellum. Prog Neurobiol. 2003; 70(6): 473–507. [PubMed: 14568361]

Sarna JR, Larouche M, Marzban H, Sillitoe RV, Rancourt DE, Hawkes R. Patterned Purkinje cell degeneration in mouse models of Niemann-Pick type C disease. J Comp Neurol. 2003; 456(3): 279–291. [PubMed: 12528192]

Sanchez M, Sillitoe RV, Attwell PJE, Ivarsson M, Rahman S, Yeo CH, Hawkes R. Compartmentation of the rabbit cerebellar cortex. J Comp Neurol. 2002; 444(2):159–173. [PubMed: 11835188]

Seil FJ, Johnson ML, Hawkes R. Molecular compartmentation expressed in cerebellar cultures in the absence of neuronal activity and neuron-glial interactions. J Comp Neurol. 1995; 356(3):398–407. [PubMed: 7642801]

Sekiguchi M, Abe H, Shimai K, Huang G, Inoue T, Nowakowski RS. Disruption of neuronal migration in the neocortex of the *dreher* mutant mouse. Dev Brain Res. 1994; 77(1):37–43. [PubMed: 8131261]

Sekiguchi M, Shimai K, Guo H, Nowakowski RS. Cytoarchitectonic abnormalities in hippocampal formation and cerebellum of *dreher* mutant mouse. Dev Brain Res. 1992; 67(1):105–112. [PubMed: 1638738]

Sgaier SK, Millet S, Villanueva MP, Berenshteyn F, Song C, Joyner AL. Morphogenetic and cellular movements that shape the mouse cerebellum; insights from genetic fate mapping. Neuron. 2005; 45(1):27–40. [PubMed: 15629700]

Sillitoe RV, Benson MA, Blake DJ, Hawkes R. Abnormal dysbindin expression in cerebellar mossy fiber synapses in the mdx mouse model of Duchenne muscular dystrophy. J Neurosci. 2003; 23(16):6576–6585. [PubMed: 12878699]

Sillitoe RV, Hawkes R. Whole-mount immunohistochemistry: a high-throughput screen for patterning defects in the mouse cerebellum. J Histochem Cytochem. 2002; 50(2):235–244. [PubMed: 11799142]

Sillitoe RV, Joyner AL. Morphology, molecular codes, and circuitry produce the three-dimensional complexity of the cerebellum. Annu Rev Cell Dev Biol. 2007; 23:549–577. [PubMed: 17506688]

Sillitoe RV, Marzban H, Larouche M, Zahedi S, Affanni J, Hawkes R. Conservation of the architecture of the anterior lobe vermis of the cerebellum across mammalian species. Prog Brain Res. 2005; 148:283–297. [PubMed: 15661197]

Sillitoe RV, Stephen D, Lao Z, Joyner AL. Engrailed homeobox genes determine the organization of Purkinje cell sagittal stripe gene expression in the adult cerebellum. J Neurosci. 2008; 28(47): 12150–12162. [PubMed: 19020009]

Smeyne RT, Goldowitz D. Purkinje cell loss is due to a direct action of the *weaver* gene in Purkinje cells: evidence from chimeric mice. Dev Brain Res. 1990; 52(1-2):211–218. [PubMed: 2331788]

Spassky N, Han YG, Aguilar A, Strehl L, Besse L, Laclef C, Ros MR, Garcia-Verdugo JM, Alvarez-Buylla A. Primary cilia are required for cerebellar development and Shh-dependent expansion of progenitor pool. Dev Biol. 2008; 317(1):246–259. [PubMed: 18353302]

Voogd J, Ruigrok TJH. Transverse and longitudinal patterns in the mammalian cerebellum. Prog Brain Res. 1997; 114:21–37. [PubMed: 9193136]

Wang VY, Rose MF, Zoghbi HY. Math1 expression redefines the rhombic lip derivatives and reveals novel lineages within the brainstem and cerebellum. Neuron. 2005; 48(1):31–43. [PubMed: 16202707]

Wassef M, Sotelo C, Thomasset M, Granholm AC, Leclerc N, Rafrafi J, Hawkes R. Expression of compartmentation antigen zebrin I in cerebellar transplants. J Comp Neurol. 1990; 294(2):223–234. [PubMed: 2332530]

Walther EU, Dichgans M, Maricich SM, Romito RR, Yang F, Dziennis S, Zackson S, Hawkes R, Herrup K. Genomic sequences of aldolase C (Zebrin II) direct lacZ expression exclusively in non-neuronal cells of transgenic mice. Proc Natl Acad Sci U S A. 1998; 95(5):2615–2620. [PubMed: 9482935]

Wingate RJ, Hatten ME. The role of the rhombic lip in avian cerebellum development. Development. 1999; 126(20):4395–4404. [PubMed: 10498676]

Zagrebelsky M, Rossi F, Hawkes R, Strata P. Topographically organised climbing fibre sprouting in the adult mammalian cerebellum. Eur J Neurosci. 1996; 8(5):1051–1054. [PubMed: 8743752]

Zhao Y, Sheng HZ, Amini R, Grinberg A, Lee E, Huang S, Taira M, Westphal H. Control of hippocampal morphogenesis and neuronal differentiation by the LIM homeobox gene Lhx5. Science. 1999; 284(5417):1155–1158. [PubMed: 10325223]

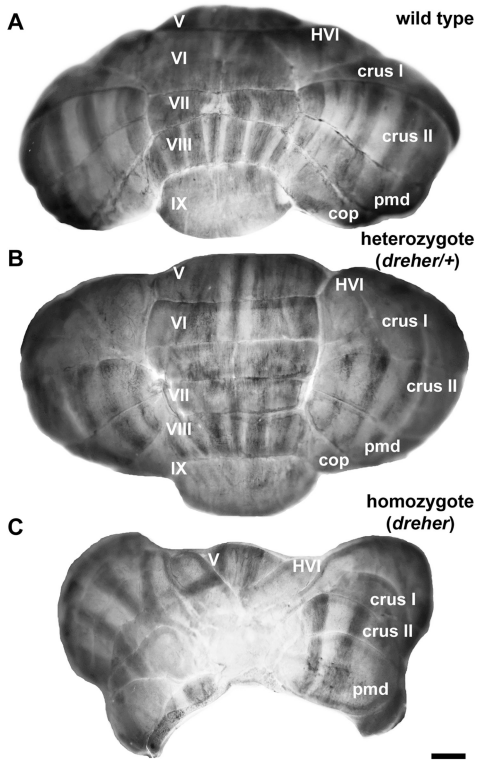

Figure 1.

The arrangement of zebrin II immunoreactive parasagittal stripes in the cerebella of littermate wild type, heterozygous and homozygous *dreher* mutant mice, shown in wholemount. **(A)** The posterior lobe vermis of a +/+ cerebellum immunoperoxidase-stained for anti-zebrin II. Zebrin II is expressed by a series of parasagittal stripes of Purkinje cells in the vermis and hemispheres of the posterior cerebellum. **(B)** The posterior lobe vermis of a cerebellum from a heterozygous animal immunoperoxidase-stained for anti-zebrin II. The expression of zebrin II is normal in the vermis and the hemispheres. **(C)** The posterior lobe vermis of a cerebellum from a homozygous *dreher* animal immunoperoxidase-stained for anti-zebrin II. The posterior lobe vermis is almost completely absent from the midline and is replaced by an ectopic mass of tissue. The hemispheric lobules are irregularly shaped but relatively correctly positioned. Zebrin II is expressed in parasagittal stripes in the hemispheres. Note that despite its small size, the vermis of lobule V is positioned normally. The vermis of the rostral aspect of lobule VI is present but deflected laterally and only partially fused at the midline. As in control and heterozygous cerebella, the expression of zebrin II in lobules V-VI in the homozygous *dreher* cerebellum reflects the AZ to CZ transition. Roman numerals indicate cerebellar lobules. Scale bar in C = 1 mm (also applies to A and B).

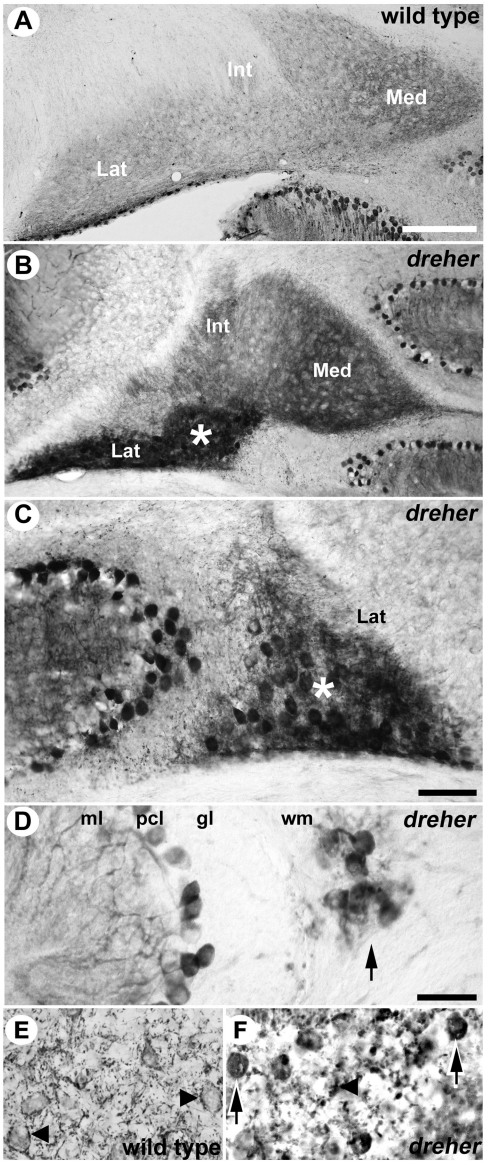

Figure 2.

Ectopic Purkinje cells are located in the cerebellar nuclei (CN) and white matter tracts of the *dreher* cerebellum. **(A)** In wild type mice Zebrin II immunoreactive axons of Purkinje cells are observed within the CN. **(B)** In *dreher* the medial (Med), intermediate (Int), and lateral (Lat) nuclei are clearly distinguished on transverse sections immunoperoxidase-stained for zebrin II. Ectopic Purkinje cell somata located in the lateral nucleus are immunoreactive for zebrin II (white asterisk). **(C)** An example of an ectopic zebrin II immunopositive cluster of Purkinje cells shown at higher magnification (the center of the cluster is labeled with a white asterisk). **(D)** An example of an ectopic HSP25 immunopositive cluster of Purkinje cells (arrow), shown at high magnification. **(E)** In wild type mice calbindin immunoreactive Purkinje cell axon terminals outline the somata of their target CN neurons (arrowheads). **(F)** In *dreher* ectopic calbindin immunopositive Purkinje cell somata (arrows) are interspersed among the CN neurons, which are outlined by immunoreactive Purkinje cell axon terminals

(arrowhead). Note that zebrin II, HSP25 and calbindin are expressed by Purkinje cells but are not expressed by the CN neurons. Scale bar in A = 250 μm (applies to B); C = 100 μm; D = 50 μm (applies to E and F).

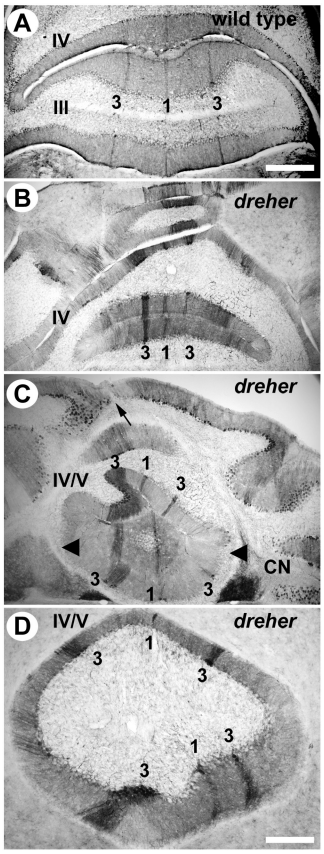

Figure 3.

Zebrin II is expressed in parasagittal stripes in the anterior zone (AZ) vermis of *dreher* mice. **(A)** At least three zebrin II immunopositive stripes are reproducible in the AZ of +/+ cerebella. In lobule III, P1+ is located at the midline and is heavily reactive for zebrin II. Two P3+ stripes are located approximately 500 μm lateral to P1+ and are also heavily reactive for zebrin II. P1- is broad and is located directly between P1+ and P3+. In lobule IV, P1- tapers and the distance between P1+ and P3+ are reduced accordingly. **(B)** In *dreher*, P1+ is central and is flanked by two P3+ stripes located 400-500 μm laterally. The width of P1- is considerably reduced. **(C)** In lobule IV, zebrin II immunopositive stripes appear deflected from the midline of the cerebellum. The zebrin II P1+ stripe and the morphological midline seen from lobules at the cerebellar surface (arrow) are not aligned. Despite the twisting of the stripes, which no longer run parasagitally, the distance between them is relatively normal. Irregularities are observed in the width of individual stripes (e.g., the P3+ stripe on the left side is wider at this level of the AZ in this individual and the P1- on the left is concomitantly reduced. **(D)** Higher magnification view of lobules IV/V, illustrating the twisted architecture of the AZ stripes P1+ and P3+. Roman numerals indicate cerebellar lobules. Scale bar = 500 μm in A (also applies to B and C); 250 μm in D.

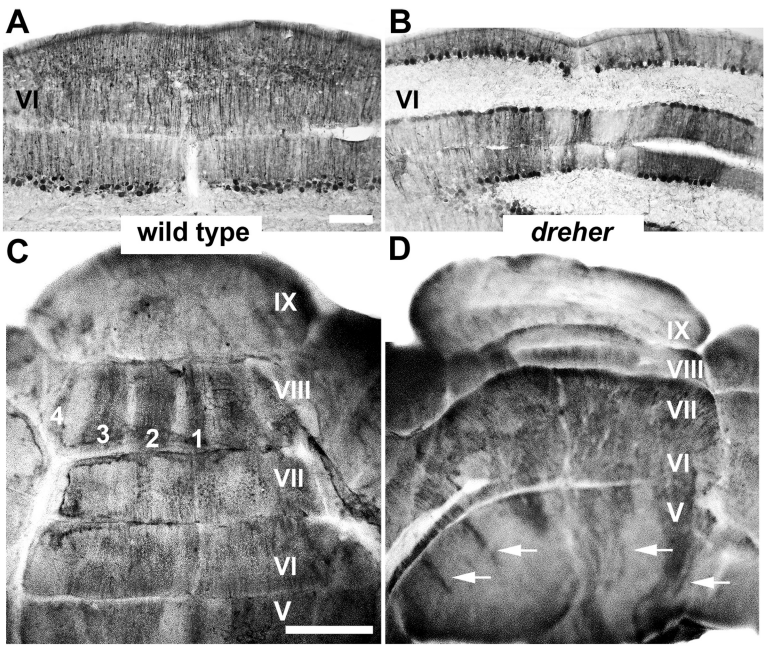

Figure 4.

Zebrin II is expressed by all Purkinje cells of the central zone (CZ) vermis in the cerebellum of *dreher* mice. **(A, C)** In the +/+ CZ, peroxidase reaction product is evenly deposited in all Purkinje cells, revealing a single uniform domain of zebrin II expression. **(B, D)** In the *dreher* CZ, most Purkinje cells express zebrin II. As in control cerebella, the transition from the AZ to CZ occurs between lobules V and VI as the regular array of stripes in the caudal AZ (arrows in D) gives way to a solid domain of expression in the rostral CZ. However, compared to the relatively central location of vermian lobule V, the vermis of lobule VI in *dreher* is deflected laterally and is located within the hemispheres. Roman numerals indicate cerebellar lobules. Scale bars = 75 μm in A (also applies to B); C = 1 mm (applies to D).

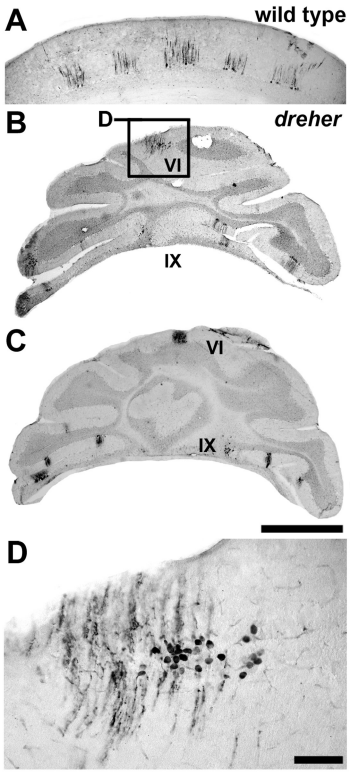

Figure 5.

The expression of HSP25 reveals parasagittal stripes in the central zone (CZ) of *dreher* mice. **(A)** HSP25 is expressed by at least five immunoreactive stripes (one stripe located at the midline and two on either side bilaterally) in the CZ of +/+ mice. **(B)** In dreher, stripes of HSP25 expressing Purkinje cells are detected in the vermis of the CZ and the NZ. **(C)** A near adjacent tissue section to the one shown in panel (B) illustrating the staggered architecture of the HSP25 pattern. The CZ stripe in this panel is more medial than the CZ stripe in panel (B). (**D**) An example of an HSP25 immunoreactive stripe in the lateral aspects of the dreher CZ (higher magnification of the box labeled C in panel B). Roman numerals indicate cerebellar lobules. Scale bars = 1 mm in C (applies to B and = 500 μm in A); D = 75 μm.

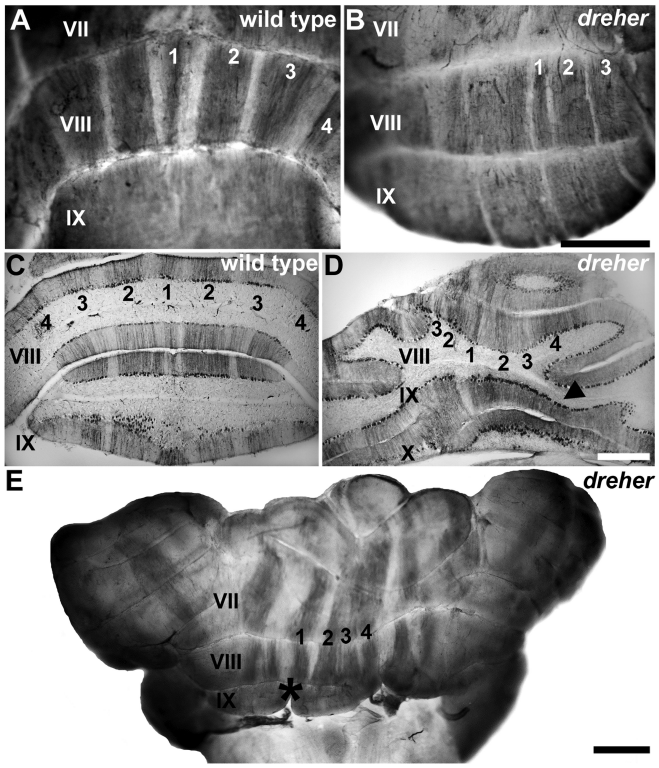

Figure 6.

Zebrin II is expressed in parasagittal stripes in the posterior zone (PZ) vermis of *dreher* mice. **(A)** Wholemount anti-zebrin II immunoperoxidase staining of control cerebella reveals an array of parasagittal stripes in the vermis of lobule VIII. **(B)** In *dreher*, wholemount immunoperoxidase-staining for anti-zebrin II reveals clearly delineated parasagittal stripes in the vermis of lobules VIII. **(C)** An example of a transverse section through the PZ of a control cerebellum immunoperoxidase-stained for zebrin II. **(D)** An example of a transverse section through the PZ of a *dreher* cerebellum immunoperoxidase-stained for zebrin II. Zebrin II immunoreactive stripes in the vermis of lobule VIII are deflected to one side of the cerebellum. **(E)** Despite abnormal foliation and abnormal fusion of the posterior vermis (e.g. lobule IX in this cerebellum) in *dreher*, an array of parasagittal stripes occupies the presumptive lobule VIII. The pattern of zebrin II in the hemispheres is distinguishable from the pattern in the vermis. The midline of the *dreher* cerebellum was often identified by a conspicuous gap in the cerebellar cortex (asterisk). Roman numerals indicate cerebellar lobules. P1+ to P4+ are labeled as 1-4 in all panels. Scale bar = 1 mm in B (also applies to A); D = 500 μm (also applies to C); E = 1 mm.

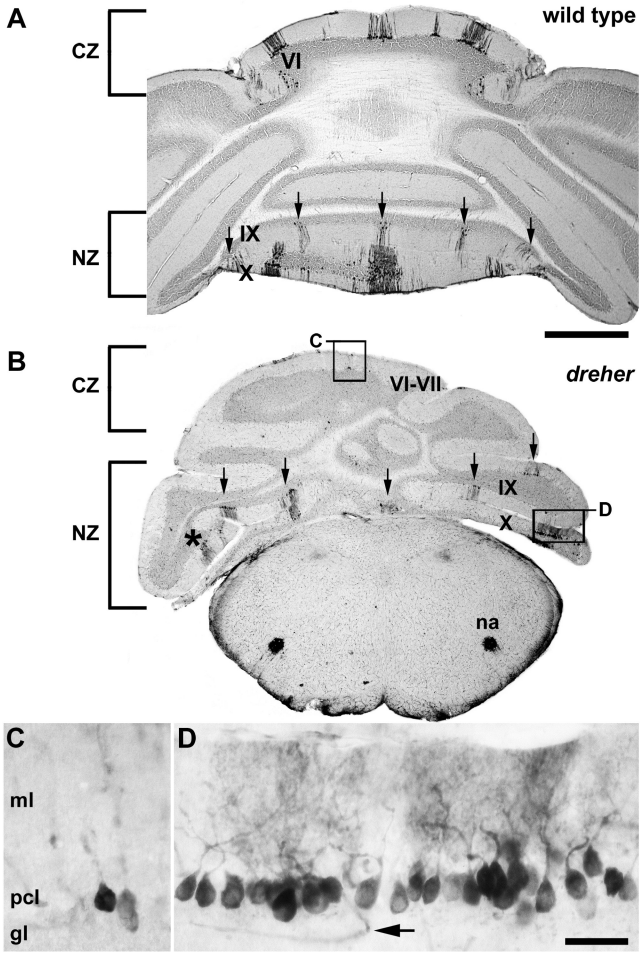

Figure 7.

The expression of HSP25 reveals parasagittal stripes in the nodular zone (NZ) of *dreher* mice. Similar to wild type mice **(A),** at least five HSP25 immunoreactive stripes are detected in lobules IX and X of *dreher* mice **(B)**. One stripe is located at the midline and is flanked by two stripes bilaterally (arrows). Note that despite the different rostrocaudal locations of each hemi-vermis, five obvious HSP25 immunoreactive stripes are visible in a single plane. **(C)** Despite the lateral deflection of lobules, stripes in the caudal CZ are fully differentiated from the stripes in the NZ (higher magnification of the box labeled C in panel B). **(D)** An example of an individual immunoreactive stripe showing that HSP25 immunoreactive Purkinje cells are organized into a monolayer (higher magnification of the box labeled D in panel B). As in control cerebella, reaction product is heavily deposited in the Purkinje cell somata and dendrites. The arrow points to an immunoreactive blood vessel in the granular layer (for details see Armstrong and Hawkes 2001). Roman numerals indicate cerebellar lobules. Scale bar = 1 mm in A (also applies to B); D = 50 μm (also applies to C).

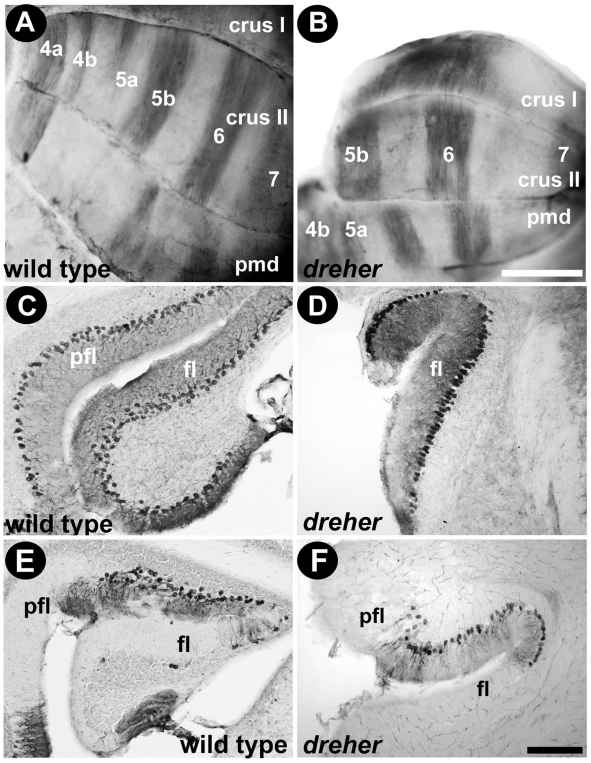

Figure 8.

Zebrin II expression reveals parasagittal stripes in the hemispheres of *dreher* mice. **(A)** In control cerebella, at least six zebrin II immunopositive stripes occupy the hemispheres (P4a +, P4b+, P5a+, P5b+, P6+ and P7+). The broad P5b+ and P6+ are heavily reactive and are easiest to identify on whole mount immunoperoxidase-stained cerebella. **(B)** P5b+ and P6+ are the most obvious stripes in the hemispheres of the *dreher* cerebellum as seen on whole mount immunoperoxidase-stained cerebella: P4+ and P7+ are resolved with less clarity. **(C)** In control cerebella zebrin II is expressed in all Purkinje cells in the flocculus (see also Eisenman and Hawkes 1993). **(D)** Zebrin II is also expressed in all Purkinje cells the *dreher* cerebellum. **(E)** In wild type cerebella HSP25 is expressed in a subset of Purkinje cells in the flocculus/paraflocculus complex (pfl/fl; for details see Armstrong and Hawkes 2001). **(F)** An example of an HSP25 immunoperoxidase-stained transverse section through the flocculus/paraflocculus in *dreher* showing that HSP25 is expressed by a subset of Purkinje cells in the paraflocculus. Scale bar = 1 mm in A (also applies to B); 50 μm in F (also applies to C, D, E).

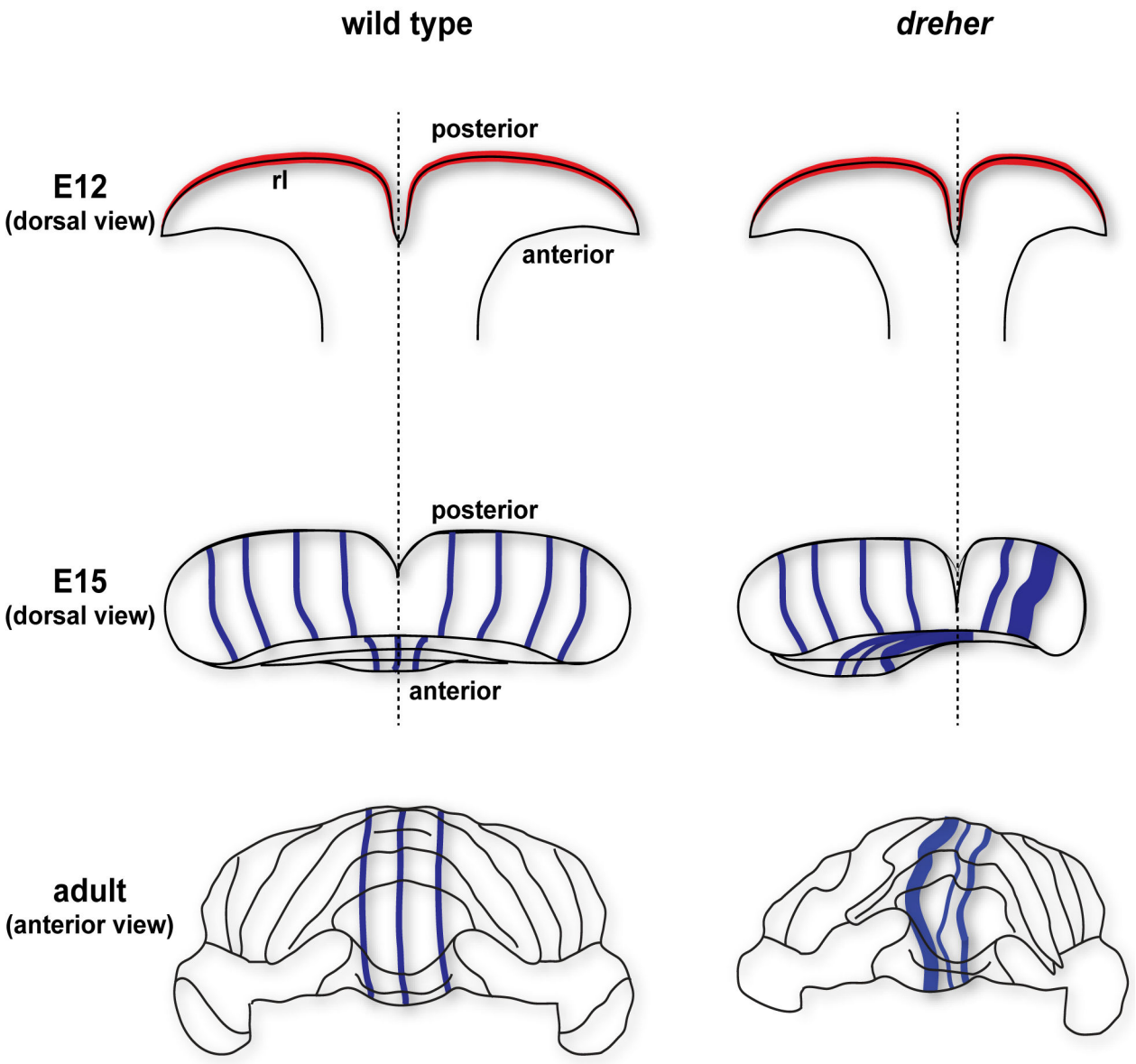

Figure 9.

Schematics illustrating three stages of cerebellar morphogenesis in wild type and *dreher* mutant mice. The rhombic lip (rl), the region that is initially affected after loss of *Lmx1a* gene expression in *dreher*, is marked in red. The blue lines in the E15 and adult schematics illustrate Purkinje cell stripe patterns. The cerebellar midline is indicated by the black dotted line. Note that the vermis (e.g. in the anterior cerebellum) is shifted laterally in *dreher* and the pattern of stripes is deflected accordingly. Because the severity of *dreher* defects is grade specific (Mishima et al. 2009), the extent of stripe deflection is variable (a mild rotation is illustrated here).